Biophysical Chemistry 3 (1975) 206–214

A PHENOMENOLOGICAL THEORY OF ROCKET IMMUNOELECTROPHORESIS [1]

John R. CANN
Department of Biophysics and Genetics, University of Colorado Medical Center, Denver, Colorado 80220, USA

Received 10 March 1975

A phenomenological theory of mass transport for antigen–antibody reactions predicts many of the characteristic features of rocket-immunoelectrophoretic patterns including the linear dependence of rocket height upon antigen concentration. The results of the calculations also have implications for the interpretation of crossed immunoelectrophoretic patterns.

1. Introduction

Although the original immunoelectrophoretic method of Grabar and Williams [1–3] has found wide application to the detection, characterization and identification of antigens, it is primarily a qualitative technique. Relatively recent immunoelectrophoretic innovations, however, permit quantitation of components in complex mixtures. Among these new methods the most promising are those of Laurell, based on electrophoresis of antigen into antibody-containing agarose gel, crossed immunoelectrophoresis [3–5] and rocket immunoelectrophoresis [6,7].

Rocket immunoelectrophoresis is a one-dimensional method in which a solution of antigen is initially placed in a well, located in a thin film of antibody-containing agarose gel molded onto a glass backing. Consider the case of a homogeneous antigen and its monospecific antiserum. Under the influence of an applied electric field the antigen migrates out of the well and through the agarose. The antibody does not migrate significantly since the operating pH (8.2–8.6) is close to its isoelectric point. As the antigen molecules migrate through the gel they react with antibody molecules to form soluble antigen–antibody complexes and specific precipitate. Migration proceeds until all the antigen has been precipitated. The resulting immunoelectrophoretic pattern consists of an open-looped line of precipitate having the shape of a rocket pointed in the direction of migration (see figs. 1 and 11B in ref. [7]). The region within the rocket can also contain precipitate (fig. 12 and accompanying discussion in ref. [7]). The height of the rocket is linearly dependent upon the initial antigen concentration other things held constant. If the test sample in the well contains two antigens with different electrophoretic mobilities and the antiserum in the gel contains antibodies to the two antigens, the immunoelectrophoretic pattern will consist of two lines of precipitate corresponding to the two antigen–antibody systems, one line of precipitate located within the other to give a double rocket (figs. 3 and 4 in ref. [7]).

Crossed immunoelectrophoresis is a two-dimensional variant of rocket immunoelectrophoresis. A mixture of antigens is first separated by simple zone electrophoresis in agarose or starch and then the separated antigens are driven through a film of agarose containing multispecific antiserum by an electric field applied at right angles to the initial separation. Each antigen gives a line of precipitate which turns on itself to form a bell-shaped peak pointed in the direction of migration. Sometimes the region within the peak contains precipitate. The resulting immunoelectrophoretic pattern consists of a set of discrete but overlapping precipitation peaks, the area under any given peak being proportional to the concentration of the corresponding

[1] Supported in part by Research Grant 5 R01 HL13909-23 from the National Heart and Lung Institute, National Institutes of Health, US Public Health Service. This publication is no. 622 from the Department of Biophysics and Genetics, University of Colorado Medical Center, Denver, Colorado 80220, USA

antigen in the initial mixture. Resolution is very high, as many as 37 peaks being detected with human serum and goat antiserum to whole human serum (see fig. 26 in ref. [3]). Identification of many of the peaks is difficult, but the use of monospecific antiserum permits detection, quantitation of individual components, and identification of specific gene products; e.g., α_1 antitrypsin (see figs. 1 and 2 in ref. [8]).

Crossed immunoelectrophoresis has been applied to the estimation of plasma proteins in pathological conditions; the analysis of microheterogeneity of purified proteins; and the demonstration of complex formation between proteins and small molecules. Rocket immunoelectrophoresis is useful for monitoring fractionation procedures. Both methods are used to screen for human α_1 antitrypsin in studies on the etiology of emphysema [9,10]. These important applications point up the need for a theory of mass transport of antigen–antibody systems which predicts rocket- and crossed-immunoelectrophoretic behavior. A phenomenological theory of rocket immunoelectrophoresis is presented in this paper.

2. Choice of a model for the precipitin reaction

The properties of the specific precipitation of antigen and antibody (precipitin reaction) can be understood qualitatively in terms of the framework theory of Marrack [11]. According to the framework theory, which biophysical studies have shown to be essentially correct [12,13], reaction of an f-valent antigen, Ag, with its homologous bivalent antibody, Ab, in the limit of infinite antigen excess leads to the formation of the single soluble complex, Ag_2Ab. The solubility of Ag_2Ab explains the antigen-excess inhibition of precipitation observed with both horse and rabbit antibody systems. In the limit of infinite antibody excess the single complex, $AgAb_f$, is formed. The fact that antibody-excess inhibition of precipitation is more readily demonstrable with horse than with rabbit antisera is usually attributed to a greater solubility of $AgAb_f$ in horse antibody systems. In any case, as antigen–antibody equivalence is approached from either antibody or antigen excess, specific complexes grow in size and eventually become insoluble so that precipitation of a three-dimensional framework of alternating antigen and antibody molecules ensues.

Several quantitative theories of the precipitin reaction have been set forth [14–19]. Of these, the theory of Goldberg [19] has been the most successful in accounting for the features of the reaction, but the number of soluble antigen–antibody complexes of different compositions (e.g., AgAb, Ag_2Ab, $AgAb_2$, Ag_2Ab_2, Ag_3Ab_2, Ag_4Ab_3, etc.) postulated to be in equilibrium with the precipitate is too large to permit formulation of a mathematically tractable theory of their interconversion during transport by electromigration and diffusion. Accordingly, we have adapted a simplified model proposed by Pauling et al. [17,18]. This model assumes an idealized antigen–antibody system consisting of a solution containing Ag molecules, Ab molecules, soluble complex molecules Ag_2Ab, and molecules AgAb of limited solubility, s, in equilibrium with precipitated compound AgAb(pp). Other antigen–antibody complexes are ignored as is the known heterogeneity of antibody molecules in serum. It is further assumed that each of the two bonds in Ag–Ab–Ag is equal in strength to the bond in Ag–Ab so that the equilibrium constants for the two homogeneous reactions in solution,

$$Ag + Ab \rightleftharpoons AgAb \qquad (1)$$

and

$$Ag + AgAb \rightleftharpoons Ag_2Ab\ , \qquad (2)$$

are $4K$ and K, respectively. Mass-action expressions for the equilibrium concentrations of Ag, Ab, AgAb, Ag_2Ab and AgAb(pp) are readily derived as functions of s, K; constituent antigen concentration, $\bar{A}$; and constituent antibody concentration, $\bar{B}$.

3. Formulation of the theory

Theoretical rocket immunoelectrophoretic patterns have been computed by numerical solution of the appropriate set of transport equations for constituent antigen and constituent antibody. The computations are for the limiting case of rates of reaction so fast that, in effect, there is local equilibrium among Ag, Ab, AgAb, Ag_2Ab and AgAb(pp). The salient features of the calculation are as follows: Suppose that a two-dimensional rectangular space grid with grid spacings, Δx and Δy, is introduced on the film of agarose gel. A small rectangular array of grid points in the space

grid represents the well, cut out of the agarose gel. Initially, only Ag at a specified concentration is present in the segments representing the well; and only Ab at its specified concentration is present in all of the other segments of the space grid. Migration in the electric field is taken to occur in the x direction with diffusion in both the x and y direction. During the first short interval of time, Δt, following application of the electric field we calculate the change in distribution of Ag and Ab due to transport. It is assumed that no reaction occurs during Δt, Ag and Ab migrating and/or diffusing independently of their initial distribution. After the concentrations have been advanced, the equilibrium concentrations of Ag, Ab, AgAb, Ag_2Ab and AgAb(pp) in each segment are calculated from the appropriate mass-action expressions. We then compute the change in this equilibrium distribution of material due to independent transport of the several species during the next Δt; recalculate the equilibrium for known constituent concentrations of antigen and antibody computed from the concentrations of the several species as changed by transport; and so on. This recursive calculation constructs the entire evolution of the distribution of material in the film of agarose gel from the initial conditions.

The rates of change of the concentrations due to independent transport are given by the conservation equations

$$\partial C_i/\partial t = D_i\,\partial^2 C_i/\partial x^2 + D_i\,\partial^2 C_i/\partial y^2 - v_i\,\partial C_i/\partial x \quad (3a)$$

for the species Ag, Ab, AgAb and Ag_2Ab ($i = 1, 2, 3$, and 4, respectively); and

$$\partial C_5/\partial t = 0 \quad . \quad (3b)$$

for AgAb(pp). In these equations, C designates concentration in moles per arbitrary units of volume; D, diffusion coefficient; and $v_i = \mu_i E$, the driven velocity in the x direction where μ_i is the electrophoretic mobility of the ith species and E is the electric-field strength. These equations have been solved in a frame of reference moving with one half the velocity of Ag, which introduces the new position variable, $x' = x - (\frac{1}{2})v_1 t$. Eqs. (3a) and (3b) are transformed into the moving coordinate systems by making the replacements $x' \to x$ and $v_i - (\frac{1}{2})v_1 \to v_i$, and adding the transport term $(\frac{1}{2})v_1\,\partial C_5/\partial x'$ to the right hand side of eq. (3b).

We now introduce discrete time and position variables

$$t_n = n\Delta t \qquad n = 0, 1, 2, \cdots,$$

$$x'_l = l\Delta x' \qquad l = 0, 1, 2, \cdots, L,$$

$$y_j = j\Delta y \qquad j = 0, 1, 2, \cdots, J,$$

and replace the continuous variable $C_i(t, x', y)$ and $C_5(t, x', y)$ by the discrete variables $C_i(n\Delta t, l\Delta x', j\Delta y) \equiv C_i(t_n, x'_l, y_j)$ and $C_5(n\Delta t, l\Delta x', j\Delta y) \equiv C_5(t_n, x'_l, y_j)$. Proceeding as in a previous investigation [20] the transformed eqs. (3a) are approximated by the finite difference equations

$$\begin{aligned} C_i(t_{n+1}, x'_l, y_j) &= C_i(t_n, x'_l, y_j) \\ &+ [D_i\,\Delta t/(\Delta x')^2]\,\{C_i(t_n, x'_{l+1}, y_j) - 2C_i(t_n, x'_l, y_j) \\ &\qquad + C_i(t_n, x'_{l-1}, y_j)\} \\ &+ [D_i\,\Delta t/(\Delta y)^2]\,\{C_i(t_n, x'_l, y_{j+1}) - 2C_i(t_n, x'_l, y_j) \\ &\qquad + C_i(t_n, x'_l, y_{j-1})\} \\ &- \{[v_i - (\tfrac{1}{2})v_1]\,\Delta t/\Delta x'\}\,[\delta C_i]_{\text{for}} \qquad i = 1, 2, 3, 4, \end{aligned} \quad (4a)$$

in which

$$\begin{aligned} [\delta C_i]_{\text{for}} &= C_i(t_n, x'_l, y_j) - C_i(t_n, x'_{l-1}, y_j) \\ &\qquad \text{if} \quad [v_i - (\tfrac{1}{2})v_1] > 0\,. \\ &= C_i(t_n, x'_{l+1}, y_j) - C_i(t_n, x'_l, y_j) \\ &\qquad \text{if} \quad [v_i - (\tfrac{1}{2})v_1] < 0\,. \end{aligned}$$

Eq. (3b) is differenced similarly. Given values of C_i and C_5 at any time, t, we can calculate their values at $t + \Delta t$ as changed by transport using these equations.

At each time, t_{n+1}, new values of the constituent concentrations of antigen and antibody are computed from C_i and C_5 as changed by transport

$$\bar{A} = C_1 + C_3 + 2C_4 + C_5\,,$$

$$\bar{B} = C_2 + C_3 + C_4 + C_5\,,$$

and then equilibrium is imposed by the following application of the law of mass action: Calculate the amount of precipitate from the equation

$$\begin{aligned} \hat{C}_5 = \bar{A} - s - [(1 + 2Ks)/(2 + 2Ks)]\,\{(\bar{A} - \bar{B}) \\ + [s(1 + Ks)/K + (\bar{A} - \bar{B})^2]^{1/2}\}\,. \end{aligned}$$

If $\hat{C}_5 \leqslant 0$:

$$\hat{C}_3 = \tfrac{1}{2}[-b + (b^2 + 2\bar{A}/K)^{1/2}] ,$$

$$b = [(1 + 2K\bar{A})^2 + 4K\bar{B}(1 - 2K\bar{A})]/8K^2\bar{B} ,$$

$$\hat{C}_1 = (\bar{A} - \hat{C}_3)/(1 + 2K\hat{C}_3) ,$$

$$\hat{C}_4 = \tfrac{1}{2}(\bar{A} - \hat{C}_1 - \hat{C}_3) ,$$

$$\hat{C}_2 = \bar{B} - \hat{C}_3 - \hat{C}_4 ,$$

$$\hat{C}_5 = 0 .$$

If $\hat{C}_5 > 0$:

$$\hat{C}_3 = s ,$$

$$\hat{C}_1 = (\bar{A} - s - \hat{C}_5)/(1 + 2Ks) ,$$

$$\hat{C}_4 = \tfrac{1}{2}(\bar{A} - \hat{C}_1 - s - \hat{C}_5) ,$$

$$\hat{C}_2 = \bar{B} - s - \hat{C}_5 - \hat{C}_4 .$$

These equilibrium concentrations, $\hat{C}_i$ ($i = 1, 2, 3, 4, 5$), serve as the starting distribution of material for the next time cycle of transport followed by re-equilibration. Given initial conditions and boundary values, this recursive calculation allows one to follow the evolution of the rocket immunoelectrophoretic pattern.

The initial conditions depend upon the initial location of the array of grid points corresponding to the antigen well. In most of the calculations the well was approximately centered in the space grid such that

$$C_1(0, x'_l, y_j) = C^0_{Ag},\ C_2(0, x'_l, y_j) = 0 ,$$

$$l = \tfrac{1}{2}(L + 1) - 21 \cdots \tfrac{1}{2}(L + 1) - 10 ,$$

$$j = \tfrac{1}{2}(J + 1) - 3 \cdots \tfrac{1}{2}(J + 1) + 2 ;$$

$$C_1(0, x'_l, y_j) = 0,\ C_2(0, x'_l, y_j) = C^0_{Ab} ,$$

$$l \neq \tfrac{1}{2}(L + 1) - 21 \cdots \tfrac{1}{2}(L + 1) - 10 ,$$

$$j \neq \tfrac{1}{2}(J + 1) - 3 \cdots \tfrac{1}{2}(J + 1) + 2 ;$$

$$C_3(0, x'_l, y_j) = C_4(0, x'_l, y_j) = C_5(0, x'_l, y_j) = 0 ,$$

$$l = 0, 1, 2, \cdots, L, \qquad j = 0, 1, 2, \cdots, J ,$$

where C^0_{Ag} is the initial concentration of Ag in the well; and C^0_{Ab}, the initial concentration of Ab in the film of agarose gel.

The boundary conditions correspond to reflection of the molecules at the edges of the space grid; i.e., $\partial C/\partial x' = 0$ and $\partial C/\partial y = 0$ at the boundaries for each species. These conditions were implemented by (1) making the following replacements just prior to each time cycle of transport

$$\hat{C}(t_n, x'_l, y_1) \to \hat{C}(t_n, x'_l, y_0) ,$$

$$\hat{C}(t_n, x'_l, y_{J-1}) \to \hat{C}(t_n, x'_l, y_J) ,$$

$$l = 1, 2, \cdots, L - 1, \quad n > 0 ;$$

$$\hat{C}(t_n, x'_1, y_j) \to \hat{C}(t_n, x'_0, y_j) ,$$

$$\hat{C}(t_n, x'_{L-1}, y_j) \to \hat{C}(t_n, x'_L, y_j) ,$$

$$j = 1, 2, \cdots, L - 1, \quad n > 0$$

for each species; and (2) integrating from $l = 1$ to $L - 1$ and $j = 1$ to $J - 1$.

We found it economical of computer time to take advantage of the transverse symmetry of the calculation. Thus, with straightforward modification of the foregoing initial and boundary conditions, integration with respect to j need only be carried over half the space grid [i.e., from $j = 1$ to $\frac{1}{2}(J - 1)$]; and the results reflected through the longitudinal line of symmetry.

Computations were made on the University of Colorado's CDC 6400 electronic computer. The values of $\Delta t = 30$–50 sec, $\Delta x' = 0.015$–0.03 cm and $\Delta y = 0.03$ cm used in these calculations satisfy a stability criterion analogous to the one used previously [20]. Driven velocities were assigned the values $v_1 = 2.8 \times 10^{-4}$, $v_2 = 0$, $v_3 = 1.4 \times 10^{-4}$ and $v_4 = 1.6 \times 10^{-4}$ cm · sec^{-1} for the calculations presented in figs. 1 and 3–7; and $v_1 = 1.04 \times 10^{-4}$, $v_2 = 0$, $v_3 = 0.52 \times 10^{-4}$, and $v_4 = 0.59 \times 10^{-4}$ cm · sec^{-1} for fig. 2. Diffusion coefficients were taken to be $D_1 = 6 \times 10^{-7}$, $D_2 = 4 \times 10^{-7}$, $D_3 = 3.68 \times 10^{-7}$, and $D_4 = 3.44 \times 10^{-7}$ cm^2 · sec^{-1}. The truncation error [21] due to the way in which the first spatial derivatives are approximated in eqs. 4 was minimized [22] in calculations made to three orders of approximation, with results which show only small quantitative differences in the direction expected for convergence. Material balance was excellent.

All calculations are for $s = 1$ and $K = 0.5$ whose dimensions are expressed in terms of moles per arbitrary unit of volume. The results are displayed as (1) maps of specific precipitate, $C_{pp} \equiv \hat{C}_5$, in the x'–y plane which correspond conceptually to experimental rocket immunoelectrophoretic patterns; (2) longitudinal and transverse distributions of the several species, e.g., $C_{Ag} \equiv \hat{C}_1$ versus x'; and (3) plots of peak height

versus t or C^0_{Ag}. 'Peak height' is the generic term for the distance from the center of the antigen well to the tip of the immunoelectrophoretic pattern of precipitation, the term 'rocket height' being reserved for fully developed patterns.

4. Results

The evolution of a theoretical rocket-immunoelectrophoretic pattern computed for initially heavy antigen excess ($C^0_{Ag}/C^0_{Ab} = 13.3$) is shown in fig. 1. It is immediately apparent that the calculation is quite predictive of experimentally observed behavior. Thus, the gross morphology of the pattern of precipitate changes during the time course of electrophoresis from that of a blunted bullet (fig. 1A–C) to that of a rocket (fig. 1D). This change in morphology is dependent upon the depletion of uncombined antigen by specific reaction with antibody, and the pattern assumes the shape of a rocket only after most (98.6%) of the antigen has reacted. The rocket shows a distinct line of maximum precipitation slightly recessed within an area of precipitation.

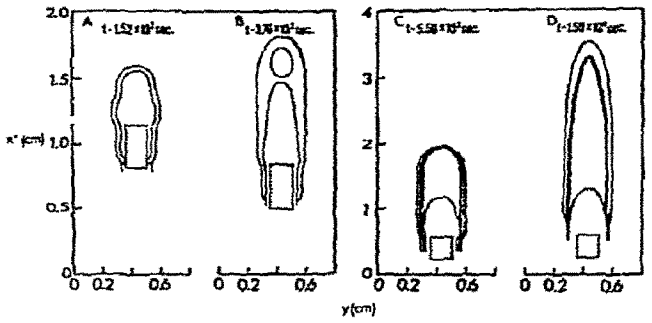

Fig. 1. Time course of development of a theoretical rocket immunoelectrophoretic pattern in heavy antigen excess, $C^0_{Ag} = 200$ and $C^0_{Ab} = 15$. Map of precipitate in the $x'-y$ plane: in this and succeeding figures showing rocket patterns the screened area is the region of precipitation; heavy line, line of maximum precipitation; and hatched area, antigen well. Time of electrophoresis is given above each pattern. Note (1) the compression of the x' scale between patterns A, B and C, D, and (2) the dependence of the position of the antigen well upon t in the moving coordinate system as well as upon its initial positioning in the $x'-y$ plane.

The detailed morphology of the theoretical pattern of specific precipitate for short times of electrophoresis is particularly provocative. As illustrated in fig. 1B, there can be an oval-shaped region devoid of precipitate located within the area of precipitation and close to its leading edge. As electrophoresis proceeds, precipitation occurs in this region (fig. 1C); but the longitudinal distribution of precipitate remains bimodal until most of the antigen has reacted and the pattern has assumed the shape of a rocket (fig. 1D). This is characteristic of patterns calculated for C^0_{Ag}/C^0_{Ab} greater than about 4 and is accentuated by increasing the ratio (fig. 2). Its explanation is given by the calculations presented in figs. 3 and 4. All of the upper half of the region within the blunted bullet presented in fig. 3A contains precipitate; but as dramatized by the relief map in fig. 3B, the precipitate is not uniformly distributed. The most striking features are the bimodal longitudinal distribution of precipitate and the resulting deep crater near the leading edge of the pattern. The longitudinal and transverse distributions displayed

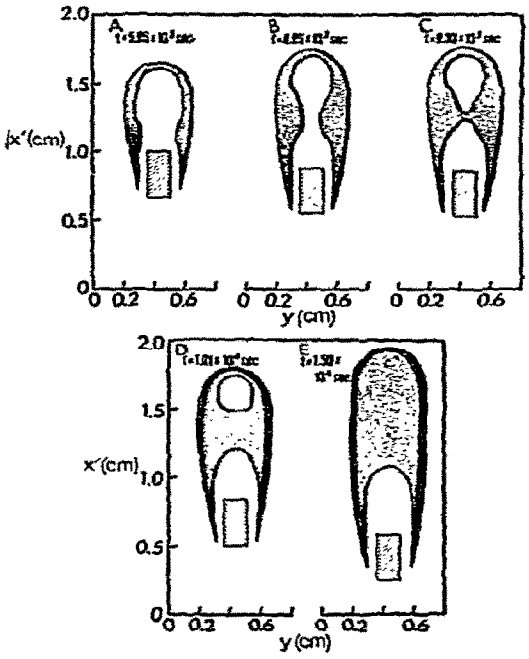

Fig. 2. Early time course of development of a theoretical rocket-immunoelectrophoretic pattern in heavy antigen excess, $C^0_{Ag} = 300$ and $C^0_{Ab} = 15$.

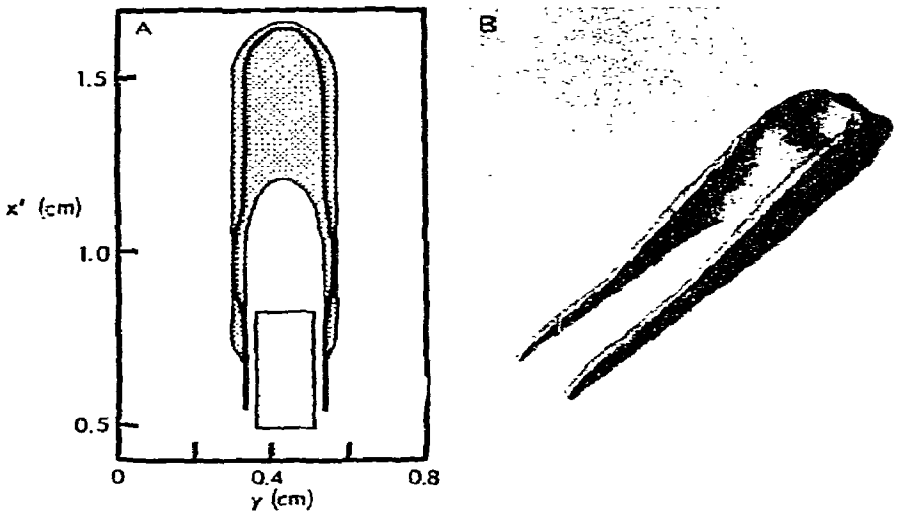

Fig. 3. Theoretical rocket-immunoelectrophoretic pattern for $C^0_{Ag} = 100$, $C^0_{Ab} = 15$ and $t = 3.78 \times 10^3$ sec: A, map of precipitate in $x'-y$ plane; B, relief map with electromigration from lower left-hand corner to upper right-hand corner and elevation proportional to the amount of precipitate.

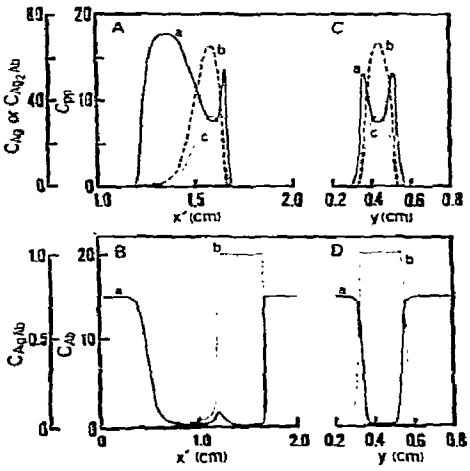

Fig. 4. Longitudinal and transverse distribution of the several interacting species for the rocket-immunoelectrophoretic pattern displayed in fig. 3. A, distributions along the longitudinal axis of the pattern: curve a, C_{pp}; b, C_{Ag}; and c, C_{Ag_2Ab}. B, distributions along the longitudinal axis: curve a, C_{Ab}; and b, C_{AgAb}. C, transverse distributions taken through the minimum of curve a in A: curve a, C_{pp}; b, C_{Ag}; and c, C_{Ag_2Ab}. D, transverse distributions through the minimum: curve a, C_{Ab}; and b, C_{AgAb}. In A and B the position of the antigen well extends from $x' = 0.49$ to 0.82 cm.

graphically in fig. 4 provide the explanation: The migrating zone of Ag is centered at the minimum of the crater which is a region of moderate antigen-excess inhibition of precipitation; and as expected there is a superimposed zone of the soluble complex, Ag_2Ab. These calculations are for $C^0_{Ag}/C^0_{Ab} = 6.7$; for larger C^0_{Ag}/C^0_{Ab} the concentration of Ag in the migrating zone is still sufficiently high at this stage of electrophoresis to give complete inhibition of precipitation so that the crater is actually a hole devoid of precipitate. This is the case in figs. 1B, 2C and 2D. The results of numerous calculations show that as electrophoresis proceeds and the region of antigen-excess inhibition of precipitation advances along with the migrating zones of Ag and Ag_2Ab, the concomitant reaction leaves behind precipitate so that the crater also advances. At the same time, the constituent concentration of antigen decreases due to both reaction and diffusion of the several species, thus approaching equivalence. Consequently, the crater becomes progressively less deep until the longitudinal distribution of precipitate loses its bimodal character and assumes an upward pitch in the region between its rapid ascent and steep decline. Along the top of the distribution $C_{pp} > C^0_{Ab}$ because antibody, bound into the complexes Ag_2Ab and, to a much lesser extent, AgAb is

transported out of the central region proximal to the antigen well and concentrated in the region where precipitation occurs (compare figs. 4A and 4B).

The coupling between the specific reactions and transport, particularly the transverse diffusion of Ag and its complexes counter to Ab, also accounts for the rocket-shaped profile of the fully developed pattern. This process can be visualized as follows: Pictorialize the zone of Ag as a relief in the $x'-y$ plane with elevation proportional to concentration. During electrophoresis, the relief erodes away due to reaction and diffusion such that its shape changes continuously from that of a tall rectangular pinnacle to a rounded-off hill with a relatively steep advancing face to a small mound until Ag virtually disappears. The composite of the time-lapse outlines of the migrating relief on the $x'-y$ plane has a rocket-shaped envelope which, in turn, determines the precipitation profile. Diffusion of Ab into the region of precipitation acts to stabilize the profile via mass action.

A set of theoretical rocket patterns for increasing initial antigen concentration at constant initial antibody concentration and time of electrophoresis is displayed in fig. 5. The increase in the height of the patterns with antigen concentration is qualitatively the same as in analogous experimental displays (e.g., fig. 1 in ref. [6] read from right to left). The plots of peak height versus time of electrophoresis shown in fig. 6

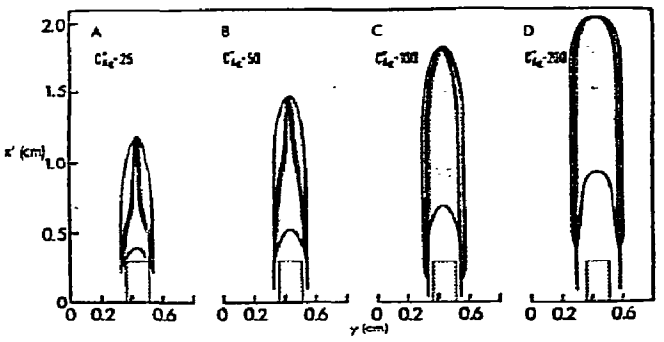

Fig. 5. Theoretical rocket immunoelectrophoretic patterns computed for increasing C^0_{Ag} at constant C^0_{Ab} = 15 and t = 7.48 × 10^3 sec. The pinched line of maximum precipitation in patterns A and B appears to reflect our assumption of instantaneous establishment of equilibrium and, to a lesser extent, the simplifying assumptions made in the model for the precipitin reaction.

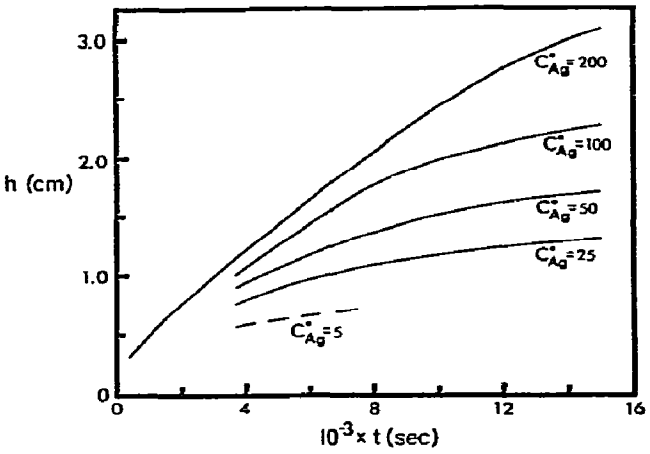

Fig. 6. Plots of theoretical peak height, h, versus t for increasing C^0_{Ag}, C^0_{Ab} = 15. The calculations for C^0_{Ag} = 5 (antibody excess of 3 to 1) (broken curve) give a small, almost stationary rocket-line pattern which on prolonged electrophoresis disappears due to solubilization of the precipitate as Ag, AgAb and Ag_2Ab at their low equilibrium concentrations migrate out of the region of precipitation. This result is to be compared to the experimental observation that when antibody is excessive a virtually stationary arc of precipitate forms close to the edge of the well.

also compare favorably with experimental curves (fig. 3 in ref. [6]), the rate of migration of the tip of the pattern decreasing with time as antigen is consumed. This is particularly striking at the relatively low antigen concentration, C^0_{Ag} = 25, for which migration almost ceases by 1.5 × 10^4 sec. Plots of peak height versus initial antigen concentration for increasing time of electrophoresis are presented in fig. 7. Once again, the general shape of the curves and their divergence are in accord with experiment (fig. 4 in ref. [6]) although they do not extrapolate to the same line at low antigen concentration. The singularly important result is shown in the insert to fig. 7; namely, for sufficiently long time of electrophoresis the height of the now fully developed rocket (more than 99% of the Ag reacted) is linearly dependent upon antigen concentration from equivalence (C^0_{Ag}/C^0_{Ab} = 1) into the region of moderately heavy antigen excess (C^0_{Ag}/C^0_{Ab} = 3.33).

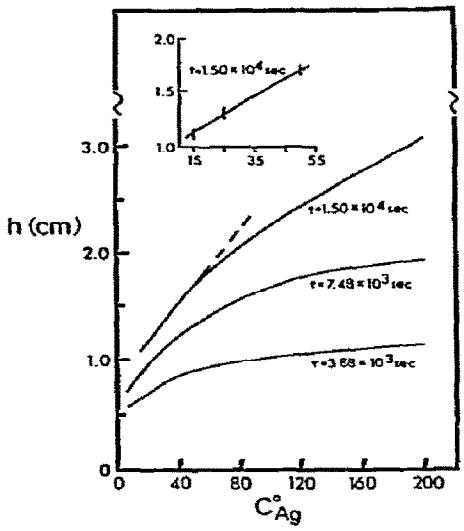

Fig. 7. Plots of theoretical peak height, h, versus C^0_{Ag} for increasing t, $C^0_{Ab} = 15$. The computed points in the insert are centered on error bars of length, $2\sqrt{2}\,\Delta x'$.

5. Discussion

The phenomenological theory described above is quite predictive of experimental observations even though the model of Pauling et al. for the precipitin reaction is highly simplified. The reason for this success of their model is that it takes cognizance of the fundamental facts that precipitating antibodies are bivalent; and that antigen-excess inhibition of precipitation is due to formation of soluble complexes, predominantly Ag_2Ab in heavy antigen excess *. Moreover, the limited solubility of AgAb also allows for inhibition of precipitation in extreme antibody excess. In short, the model embodies several of the properties of the precipitin reaction and thus predicts the general shape of the precipitin curve.

The fact that the region within calculated rockets always contains precipitate, except for the central area proximal to the well, invites comment. Although many proteins give experimental rockets characterized simply by a narrow line of precipitate; others give a distinct outer but a smudged inner demarcation; and in still other cases the rockets contain precipitate virtually throughout the region bounded by a sometimes blurred line of maximum precipitation. Also, crossed immunoelectrophoretic peaks filled with precipitate are not uncommon. Evidently, the gross appearance of a particular rocket or peak depends among other things upon the solubility of the corresponding antigen and its various complexes with antibody [7]; but the model of Pauling et al. for the precipitin reaction does not take account of all of these parameters.

The theoretical patterns of specific precipitate for short times of electrophoresis also have their experimental counterparts. Thus, Laurell has obtained rocket patterns with fibrinogen (fig. 12 in ref. [7]) having features similar to those shown by the patterns in figs. 1B and 3B; and he recognized that such morphology indicates that electrophoresis was stopped before all the antigen had been bound. He has also obtained patterns with amylase (fig. 19A in ref. [7]) reminiscent of figs. 2C and 2D, the rockets containing precipitate from the well to their somewhat rounded tips except within a large oval zone proximal to the tip. In view of our computational results, these patterns can hardly be misread. The disturbing thing, however, is that under certain conditions the complexion of the pattern might be such as to be misinterpretable in terms of antigen heterogeneity. This is more likely to be a complication of crossed immunoelectrophoresis of complex mixtures. Consider, for example, the crossed immunoelectrophoretic pattern of Timothy pollen extract which shows six precipitates (fig. 21.1 in ref. [23]). Of relevance to this discussion are the precipitates labeled 1 and 2 whose relative positioning and general appearance suggest that they might actually constitute a single, doubly contoured peak of the sort under consideration. Whenever such double peaks are encountered in practice, experiments should be done to determine the time of electrophoresis required for exhaustion of the antigen by reaction with antibody. Depending upon the outcome of such experiments, fractionation of the antigen either by isolation and dissociation of the precipitates or by some independent method may be necessary for unequivocal proof of heterogeneity.

Finally, the power of rocket immunoelectrophoresis is that it is a quantitative method of analysis for antigen, the height of fully developed rockets in-

* Arend et al. [24] have concluded that in the region of low to moderate antigen excess the smallest complex as defined operationally in the ultracentrifuge is predominantly AgAb, at least in the two systems they examined.

creasing linearly with antigen concentration other things held constant. It is gratifying, therefore, that the theory gives this relationship.

References

[1] P. Grabar and C.A. Williams, Biochim. Biophys. Acta 10 (1953) 193.
[2] P. Grabar and C.A. Williams, Biochim. Biophys. Acta 17 (1955) 67.
[3] C.A. Williams and M.W. Chase, Method in Immunology and Immunochemistry, vol. III, Reactions of Antibodies with Soluble Antigens (Academic Press, N.Y., 1971) pp. 234–294.
[4] C.-B. Laurell, Anal. Biochem. 10 (1965) 358.
[5] N.H. Axelsen, J. Knøll and B. Weeke, A Manual of Quantitative immunoelectrophoresis. Methods and Applications, Scand. J. Immunol. 2 (1973) Suppl. 1.
[6] C.-B. Laurell, Anal. Biochem. 15 (1966) 45.
[7] C.-B. Laurell, Scand. J. Clin. Lab. Invest. 29 (1972) Suppl. 124, 21.
[8] B.H. Bowman, in: Electrophoresis. Theory, Methods, and Applications, ed. M. Bier, vol. II (Academic Press, N.Y., 1967) ch. 4.
[9] M.K. Fagerhol and C.-B. Laurell, Progress in Medical Genetics 7 (1970) 96.
[10] C.-B. Laurell, Scand. J. Clin. Lab. Invest. 29 (1972) 247.
[11] J.R. Marrack, Med. Res. Council (Brit.), Spec. Rept. 230 (1938).
[12] M. Heidelberger and K.O. Pedersen, J. Expt. Med. 65 (1937) 393.
[13] S.J. Singer, in: The Proteins, vol. III, ed. H. Neurath, 2nd edition (Academic Press, N.Y., 1965) ch. 15.
[14] M. Heidelberger and F.E. Kendall, J. Expt. Med. 61 (1935) 563.
[15] F.E. Kendall, Ann. N.Y. Acad. Sci. 43 (1942) 85.
[16] A.D. Hershey, J. Immunol. 42 (1941) 455.
[17] L. Pauling, D. Pressman, D.H. Campbell and C. Ikeda, J. Am. Chem. Soc. 64 (1942) 3003.
[18] L. Pauling, D.H. Campbell and D. Pressman, Physiol. Rev. 23 (1943) 203.
[19] R.J. Goldberg, J. Am. Chem. Soc. 74 (1952) 5715.
[20] J.R. Cann and W.B. Goad, J. Biol. Chem. 240 (1965) 148.
[21] W.B. Goad and J.R. Cann, Ann. N.Y. Acad. Sci. 164 (1969) 172.
[22] J.R. Cann and G. Kegeles, Biochemistry 13 (1974) 1868.
[23] B. Weeke and H. Løwenstein, Scand. J. Immunol. 2 (1973) Suppl. 1, 147.
[24] W.P. Arend, D.C. Teller and M. Mannik, Biochemistry 11 (1972) 4063.